Journal of Magnetism and Magnetic Materials 324 (2012) 3791–3798

Contents lists available at SciVerse ScienceDirect

Journal of Magnetism and Magnetic Materials

journal homepage: www.elsevier.com/locate/jmmm

A microfluidic spiral for size-dependent fractionation of magnetic microspheres

Silvio Dutz [a,b,*], M.E. Hayden [c], Allison Schaap [d], Boris Stoeber [d,e], Urs O. Häfeli [a]

[a] Faculty of Pharmaceutical Sciences, The University of British Columbia, Vancouver, Canada
[b] Department of Nano Biophotonics, Institute of Photonic Technology, Jena, Germany
[c] Department of Physics, Simon Fraser University, Burnaby, Canada
[d] Department of Mechanical Engineering, The University of British Columbia, Vancouver, Canada
[e] Department of Electrical and Computer Engineering, The University of British Columbia, Vancouver, Canada

ARTICLE INFO

Article history:
Received 9 March 2012
Received in revised form
20 May 2012
Available online 17 June 2012

Keywords:
Magnetic microsphere
Size dependent fractionation
Lab-on-a-chip
Microfluidic

ABSTRACT

Magnetic microspheres (MMS) are useful tools for a variety of medical and pharmaceutical applications. Typically, commercially manufactured MMS exhibit broad size distributions. This polydispersity is problematic for many applications. Since the direct synthesis of monodisperse MMS is often fraught with technical challenges, there is considerable interest in and need associated with the development of techniques for size-dependent fractionation of MMS. In this study we demonstrated continuous size-dependent fractionation of sub-micron scale particles driven by secondary (Dean effect) flows in curved microfluidic channels. Our goal was to demonstrate that such techniques can be applied to MMS containing superparamagnetic nanoparticles. To achieve this goal, we developed and tested a microfluidic chip for continuous MMS fractionation. Our data address two key areas. First, the densities of MMS are typically in the range 1.5–2.5 g/cm^3, and thus they tend be non-neutrally buoyant. Our data demonstrate that efficient size-dependent fractionation of MMS entrained in water (density 1 g/cm^3) is possible and is not significantly influenced by the density mismatch. In this context we show that a mixture comprising two different monodisperse MMS components can be separated into its constituent parts with 100% and 88% success for the larger and smaller particles, respectively. Similarly, we show that a suspension of polydisperse MMS can be separated into streams containing particles with different mean diameters. Second, our data demonstrate that efficient size-dependent fractionation of MMS is not impeded by magnetic interactions between particles, even under application of homogeneous magnetic fields as large as 35 kA/m. The chip is thus suitable for the separation of different particle fractions in a continuous process and the size fractions can be chosen simply by adjusting the flow velocity of the carrier fluid. These facts open the door to size dependent fractionation of MMS.

1. Introduction

Magnetic microspheres (MMS) are being used for a variety of medical and pharmaceutical applications. They are essential for magnetic drug targeting [1] and typically consist of a polymeric matrix material, e.g., albumin, chitosan, and biodegradable polymers poly(lactic acid) (PLA) or poly(lactide-co-glycolide) (PLGA), which enclose a magnetic core, e.g., magnetite or maghemite. The MMS can also enclose a pharmaceutical agent, e.g., chemotherapeutic drugs or blood clot dissolving agents [2,3] and are often coated with (receptor) targeting agents, e.g., antibodies, peptides, and/or with agents improving their stability and blood circulation time, e.g., polyethylene glycols. After injection into the blood stream of animals and humans, MMS can be magnetically guided to a target area where the pharmaceutical agent acts on the target cells or disease after controlled release [4].

Typical MMS used for drug delivery have diameters in the range 0.1–10 μm and exhibit a lognormal size distribution [5]. In order to steer MMS effectively for drug targeting, they must be as large as possible (assuming a constant concentration of magnetic material in the MMS) because the magnetic force on an MMS is directly proportional to the volume of the magnetic material in the MMS [6]. However, there is an absolute upper limit on size of 5 μm, above which the risk of clogging (embolizing) blood capillaries is high, leading to thrombosis and significant risk of mortality for the patient [7]. Furthermore, uniform MMS size distributions are essential for the design of predictable drug

* Corresponding author at: Institute of Photonic Technology Magnetics Albert-Einstein Strasse 9, 07745 Jena Germany. Tel.: +49 3641 206317; fax: +49 3641 206139.
E-mail address: silvio.dutz@ipht-jena.de (S. Dutz).

0304-8853/$ - see front matter © 2012 Elsevier B.V. All rights reserved.
http://dx.doi.org/10.1016/j.jmmm.2012.06.014

release profiles for drug-containing MMS, since release kinetics are in general a function of the particle surface-to-volume ratio [8]. Thus, in order to guarantee optimal clinical magnetic targeting and defined drug release, MMS with uniform and consistent particle sizes are necessary.

One way to obtain appropriate particles is to directly synthesize monodisperse MMS. Some types of commercially available MMS show a relatively narrow size distribution but these particles are not biocompatible, a precondition for magnetic drug targeting. Preparing monosized particles can be technically challenging. A different route to obtaining such particles is to prepare batches of MMS with broad size distributions, and subsequently apply size dependent fractionation techniques to obtain MMS with the desired parameters.

Size dependent fractionation of magnetic particles is possible and has previously been reported. Methods include gravitational forces [9,10] and centrifugation [9,10], magnetic forces [11–14], or changing the repulsion forces between single particles by varying the zeta potential of the particles, which is controlled by means of a variation of the pH of the sample [15]. All of these methods suffer from the problem that they are suitable only for batch processing of limited sample volumes. The implication is that the quantity of fractionated material produced per batch is relatively low and thus these methods tend to be suitable only for the processing of analytical quantities.

To overcome this drawback several microfluidic methods for continuous fractionation of microparticles have been developed. The majority of these use filtration [16,17], gravity forces [18], sound pressure [19], optical forces [20], and magnetic forces [21–24] for the classification of magnetic particles. Comprehensive reviews about recent developments in this field are given by Pamme [25] and Adams and Soh [26].

An additional method that can be applied to the fractionation of particles is the Dean effect [27,28], an established flow phenomenon. The Dean effect occurs in a curved channel—a secondary flow is formed that consists of two counter rotating vortices as shown in Fig. 1. Recent research has shown that if particles are present in the flow, particles above a distinct size migrate toward the inner wall of the bend. This separation principle in curved channels has been demonstrated by several authors, who were able to focus particles of certain size to a streamline [29] or to remove fluorescent beads from human plasma [30] or filtered water [31]. Other authors have demonstrated the suitability of this method for the separation of particles into different size ranges, and have performed numerical simulations that replicate their experimental results [32,33].

Our aim was the development, construction, and testing of a microfluidic chip for the size dependent fractionation of magnetic microspheres (MMS). The previous work described above involves particles with densities similar to that of water (1 g/cm^3) to obtain neutrally buoyant behavior. MMS have a density of about twice that of water and clearly exhibit non-neutrally buoyant behavior. As previous work did not indicate whether fractionation of non-neutrally buoyant particles is possible using the Dean effect, one key task of our study was an experimental investigation of the influence of particle density on the fractionation process.

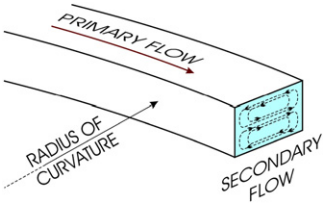

Fig. 1. In a curved channel two counter rotating Dean vortices (secondary flow) develop perpendicular to the main flow (primary flow) direction.

Beyond this, it is of practical interest to explore the question of whether or not magnetically induced agglomeration might be a problem for the fractionation of MMS via the Dean effect. For this purpose, we intentionally exposed our microfluidic chip (while the fractionation process was underway) to a homogeneous magnetic field as well as to a magnetic field gradient. MMS tend to form agglomerates in strong magnetic fields and field gradients leading to the formation of large clusters and chains which might compromise Dean effect fractionation. Here, we investigate this aggregation behavior and verify that fractionation based on the Dean effect is indeed feasible under the influence of reasonably strong magnetic fields. This observation is quite significant in that it opens the door for combining flow-based fractionation processes with intentionally-applied magnetic forces in further investigations.

2. Fundamentals

The flow-fractionation principles upon which the design of our chip is based are the Dean effect [27,28] and lift forces [34]. When a fluid flows through a curvilinear channel, a secondary flow in the form of two counter-rotating vortices develops across the channel; these are known as Dean vortices (see Fig. 1). If the fluid contains a suspension of particles, the secondary flow causes particle transport to occur across the channel (i.e., perpendicular to the primary flow) driven by Dean vortices.

The strength of the Dean flow is characterized by the dimensionless Dean number

$$D_e = \frac{\rho v_f D_h}{\eta_f}\sqrt{\frac{D_h}{2r}} \tag{1}$$

with

$$D_h = \frac{4A}{P}, \tag{2}$$

where ρ is the density of the fluid, v_f is the mean fluid velocity along the channel, η_f is the dynamic viscosity of the fluid, r is the radius of curvature of the channel, and D_h is its hydraulic diameter which is related to the cross sectional area A and the wetted perimeter P of the channel. A larger Dean number causes stronger Dean vortices.

In addition to particle transport caused by secondary flow, lift forces act on the particles. Wall-induced inertial lift forces (F_{WL}) push particles away from walls [35] while shear-induced inertial lift forces (F_{SL}) associated with the primary flow drive particles away from the center of the microchannel [34]. The former (F_{WL}) dominate when particles are close to walls and the latter (F_{SL}) dominate when particles are further away. The strength and direction of the net lift force (F_{NL}) [32] varies across the microchannel cross-section and is a function of particle size. For straight channels, particles entrained in the flow tend to aggregate at various equilibrium positions that depend on geometry. These equilibrium positions correspond to lines or surfaces (parallel to the axis of the channel) along which $F_{NL}=0$. For example, in a square or rectangular channel, particles tend to aggregate and flow along lines that are situated a short distance away from the midpoint of each face. In a cylindrical channel, they flow along sheets at a fixed distance from the wall [36]. The precise location of these lines or surfaces depends on particle size. When curvature is introduced, Dean vortices are established and impose an additional drag force (perpendicular to the primary flow) that can modify or destroy lines or surfaces of stable equilibrium. For example, in a square or rectangular channel that

is curved as shown in Fig. 1, the additional fluid circulation associated with Dean flow sweeps particles located near either the top or the bottom surfaces of the channel toward the inner wall. Similarly, there is a tendency for the secondary flow to destabilize the line of equilibrium near the outer wall that is observed for straight channels. That is, any particle that wanders away from the precise location at which the drag and lift forces cancel becomes entrained in the secondary flow and is pulled away. The only line of stable equilibrium that survives the introduction of curvature is the one located near the inner wall of the channel. Here, the tendency of the secondary flow is to drive particles toward the midpoint of the wall from above and below. While it is true that the secondary flow also tries to sweep particles away from this line of equilibrium along the transverse midline of the channel, this drag is opposed by the shear-induced lift force associated with the primary flow; the net result is simply a shift in the position of the line of equilibrium relative to the wall. Thus, for a given combination of channel geometry, flow rate, and particle diameter a single line of equilibrium close to the midpoint of the inner wall exists. Along this line, all cross-channel forces acting on these particles are in balance. Particles thus tend to accumulate at this equilibrium position and are transported along an apparent streamline of the primary flow (Fig. 2). Particle entrainment along streamlines in curved microchannels has been reported previously for Dean numbers ranging from 0.48 to 1.49 [30] and from 0.23 to 0.94 [32].

In the present investigation we developed and tested a microfluidic chip in which particles of a certain size are constrained to flow along a streamline at an equilibrium position close to the inner wall of a curved channel, and then separated the flow into two fractions: an inner fraction (containing the particles trapped at the equilibrium position) and an outer fraction containing the remaining particles. The net result is two fluid streams containing particles with different characteristic dimensions.

3. Materials and methods

3.1. Design and preparation of the chip

Fig. 3 shows the layout of the microfluidic system for MMS size fractionation using the Dean effect. It comprises an inlet port located near the center of the spiral, the spiral structure itself, a 1:1 splitter at the outer periphery of the spiral, and two outlet ports. The splitter separates the flow into two streams which are extracted via the outlet ports. These are referred to as the "inner outlet" (io) and "outer outlet" (oo) ports based on their position relative to the spiral structure.

To design a chip suitable for size dependent fractionation of MMS with diameters in the range 1–15 μm dispersed in water, a minimum channel length, suitable radius of curvature, and appropriate cross-sectional channel dimensions have to be determined. Assuming a flow rate in the range 10–50 μL/min (suitable for PDMS chips) and taking into account Eqs. (1) and (2), a hydraulic diameter of 150 μm and a spiral radius of curvature less then 8 mm yield a Dean number of order 0.5, which gives conditions under which apparent focusing of particles along streamlines has been observed by other groups [30,32].

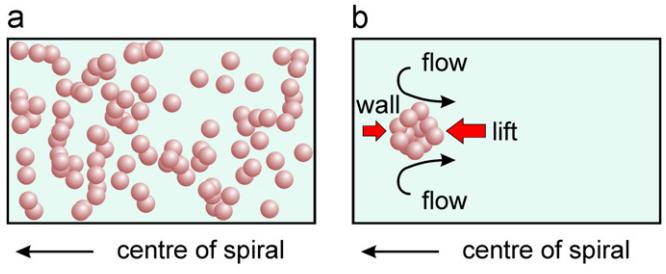

Fig. 2. Cross-section of the channel: starting from (a) an initially random particle distribution across the channel particles and (b) accumulated at an equilibrium position near the inner wall of the spiral structure. At this point the combined effects of lift and Dean drag forces acting perpendicular to the primary flow (out of the page) are balanced.

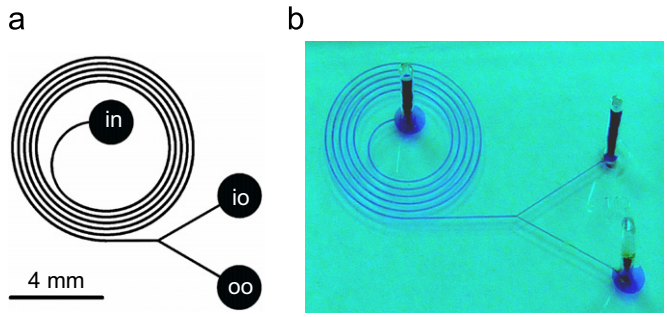

Fig. 3. (a) Schematic and (b) photograph showing the geometric layout of the fractionation system, including the positions of the inlet (in), the outer outlet (oo), and the inner outlet (io) ports. In (b) the connection tubing was removed for better visibility of the chip.

The minimum length L required for a curved microchannel to produce significant size fractionation via the Dean effect is given by

$$L = \frac{3\pi\,\eta_f}{2\rho v_f}\left(\frac{L_C}{d}\right)^3 \tag{3}$$

where d is the MMS diameter, and L_C is a characteristic length (for a channel with a rectangular cross-section, it is the shortest dimension). We selected the channel height L_C=60 μm as a convenient size for channel fabrication and thus L was determined to be at least 100 mm.

On the basis of these estimates, a set of designs for spirals with different dimensions were obtained. The channel length in these designs varied from 70 to 180 mm (4–6 turns), the radius of curvature varied from 3 to 6 mm, and the hydraulic diameter varied from 75 to 100 μm. Prototype microfluidic chips based on this set of designs were manufactured and tested to find a combination of dimensions suitable for further investigation of Dean effect-based particle fractionation. On the basis of these preliminary experiments that were conducted for flow rates in the range 10–50 μL/min, we selected a 5-turn spiral structure with an outer diameter of approximately 6 mm and a 100 μm wide by 60 μm high rectangular channel as being suitable for the fractionation of MMS with diameters ranging from 2 to 12 μm.

The microfluidic chips were made from polydimethylsiloxane (PDMS). The channel structure including the spiral, the inlet and the two outlets was first designed and drawn (Fig. 3) using CleWin4 (PhoeniX Software, Enschede, The Netherlands) and then printed on a high resolution (20,000 dpi) transparency mask (CAD/Art Services, Bandon, USA). A mould was fabricated from this transparency mask using a permanent epoxy negative photoresist (SU-8 2075, Microchem, Newton, USA). This structure then served as a mold for creating a PDMS (Sylgard 184, Dow Corning, Midland, MI, USA) cast. After curing, the PDMS was removed from the mould, inlet holes were punched at each of the three ports, and the piece was attached to a glass microscope slide (both surfaces were prepared in advance with a plasma surface activation). Finally, a 0.5 mm (inner diameter) polymer tubing was connected to each of the three ports simply by wedging the tubing into the holes.

3.2. Fractionation of microspheres

For evaluating the performance of the chip, MMS consisting of a styrene–maleic acid copolymer matrix encapsulating 50% by mass magnetite cores (MMS density = 1.85 g/cm^3) were used. Their mean diameters were 2, 4, 5, 6, 8, 10, and 12 μm (Micromer®-M, micromod Partikeltechnologie, Rostock, Germany) with relatively narrow size distribution. This set of MMS sizes allows the investigation of the separation behavior of the chip with respect to the removal of MMS larger or smaller than the desired size (5 μm). Specially prepared MMS with a broad size distribution consisting of maghemite cores (50% by mass, MMS density = 2.25 g/cm^3) in a silica matrix and silanol groups on the surface showing a mean diameter of 3.56 ± 2.82 μm (SiMAG-Silanol, chemicell, Berlin, Germany) were also used.

Micromer®-M MMS with a diameter of 5 μm and a density of 1.85 g/cm^3 and non-magnetic microspheres with the same size and a density of 1.1 g/cm^3 (Micromer®-plain, micromod Partikeltechnologie, Rostock, Germany) were used for the investigation of the influence of density on the fractionation process.

Aqueous suspensions of MMS in concentrations of 0.5% by mass were filled in a disposable syringe and pumped into the microfluidic channel by means of a BS-8000 syringe pump (Braintree Scientific, Braintree, MA, USA) with flow rates varying from 5–80 μL/min. The fractions obtained at the inner and outer outlets were collected and characterized. Experiments were carried out using a high-speed camera (Phantom Miro 4, Vision Research, Wayne, NJ, USA) attached to a microscope (Eclipse TE2000-U, Nikon, Melville, NY, USA).

The following MMS suspensions of different size and composition were tested in the chip:

A. MMS with a narrow size distribution and a diameter of 6 μm or 10 μm. The total amount of MMS extracted at the inner and the outer outlets was determined by means of a haemocytometer (Hausser Scientific, Horsham, PA, USA), and was studied as a function of flow rate.
B. A mixture of 2 μm and 12 μm diameter particles with narrow size distributions. Samples collected from the two outlets were characterized by static light scattering (Mastersizer 2000, Malvern Instruments, Malvern, UK) to determine separation efficiency as a function of flow rate.
C. Polydisperse MMS with a mean diameter of 3.5 μm. Samples extracted from the outlets were characterized by static light scattering to determine mean particle diameters and distributions as a function of flow rate.
D. Non-magnetic and magnetic microspheres with the same diameter (5 μm) but different densities (1.1 and 1.85 g/cm^3). To study the influence of particle density on fractionation efficiency, a 1:1 mixture of these particles was fractionated and the resulting distribution of magnetic versus non-magnetic components extracted from each outlet was determined by vibrating sample magnetometry (VSM, Micromag 3900, Princeton Measurement Corporation, Princeton, NJ, USA).

We confirmed that size dependent scattering intensity does not distort the obtained volume-weighted size distributions by comparing the sum of peak areas for small or large MMS in both fractions to the ratio of the number of large particles to small particles in the original sample as well as to the expected ratio calculated from the known particle concentration in the stock dispersions.

For the investigation of the influence of magnetic fields and/or magnetic field gradients on Dean fractionation, both a permanent magnet and a Helmholtz coil were used. The simplest way to investigate the influence of an inhomogeneous magnetic field (i.e., involving field gradients) on the functioning of the chip is to expose the chip to a magnetic field generated by a permanent magnet. For this, a permanent magnet (NdFeB 38, $5 \times 5 \times 11$ mm^3, axially magnetized) was placed in the plane of the spiral with the magnetic field gradient aligned in radial direction. By changing the distance between the magnet and the chip inlet, magnetic field strengths ranging from 5.5 to 50 kA/m (or magnetic flux density gradients between 1.5 and 20 T/m) were realised at the inlet of the chip. To investigate the influence of a spatially homogenous magnetic field (no field gradient) on the operation of the fractionation process, the chip was placed between a pair of coils (in a Helmholtz configuration) which generate field strengths up to 35 kA/m. Here it was of particular interest to determine whether or not the homogeneous magnetic field leads to an agglomeration of particles which could influence or disrupt particle movement in the secondary flow. The homogeneous field was applied both in plane and perpendicular to the spiral structure to examine effects related to anisotropy. In both configurations the agglomeration behavior of the MMS and the formation of Dean flow induced MMS streams were observed by means of a microscope.

4. Results and discussion

4.1. Monodisperse MMS

For experiments involving monodisperse MMS with 6 μm or 10 μm diameters, it was observed that particles were distributed homogeneously across the channel at low (5 μL/min) flow rates (Fig. 4a). With increasing flow velocity, a migration of the particles near the inner wall of the spiral was observed. For flow rates higher than 50 μL/min, a clear zone of high particle concentration was observed (Fig. 4b). All of the particles moved near the inner wall and thus towards the inner outlet and none were found in the outer fraction.

Fig. 5 shows the relative distribution of MMS collected from the inner and the outer outlets during these experiments. It is evident that the number of small- and large-diameter particles extracted from the inner and outer outlets are nearly the same at flow rates of order 5 μL/min. At flow rates of 80 μL/min, 94.3% of the 6 μm-diameter MMS and 99.5% of the 10 μm-diameter MMS were found in the inner fraction. This demonstrates that the microfluidic fractionation chip is able to recover nearly all monodisperse MMS from dilute MMS dispersions in continuous operation. As seen in Fig. 4b the enrichment of particles near the inner wall is already completed in the fourth winding; the percentage of particles in the inner fraction can therefore not be further increased by using a longer channel.

Because of the 1:1 splitter geometry and the fact that particles move to the inner wall, the concentration of particles extracted from the inner outlet is nearly double that of the initial concentration. Further increases in concentration could be achieved by reintroducing the output from the inner outlet into another microfluidic spiral (or a series of spirals). In each pass through the fractionation system the concentration of MMS would double. By repeating this process several times or cascading several identical spiral structures an enrichment of very dilute suspensions of micron-scale particles can be achieved. A larger concentration factor per chip can be achieved using an asymmetric splitter at the end of the spiral. For example: a 4-fold increase in concentration could be achieved by designing the splitter such that the cross section of the inner outlet channel is 1/3 that of the outer outlet channel. Clearly one still needs to ensure that the flow rate in the outer outlet channel is 3 times that in the inner

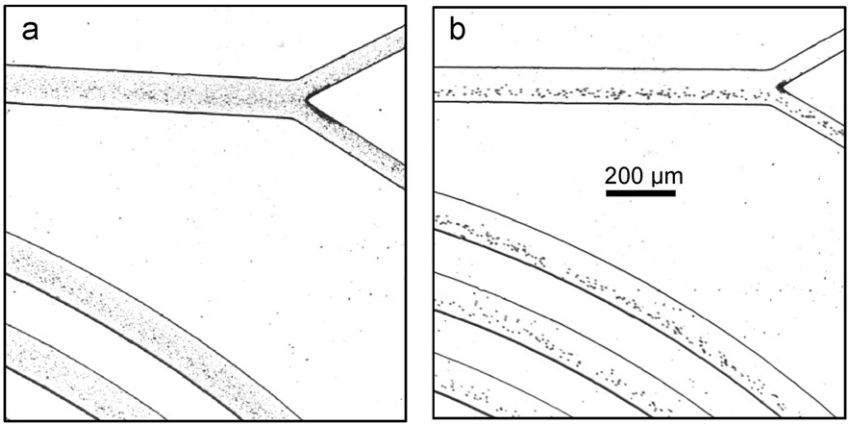

Fig. 4. Photographic picture of the microfluidic spiral containing 10 μm diameter particles with a narrow size distribution (a) at low flow rates (5 μL/min) and (b) at high (50 μL/min) flow rates.

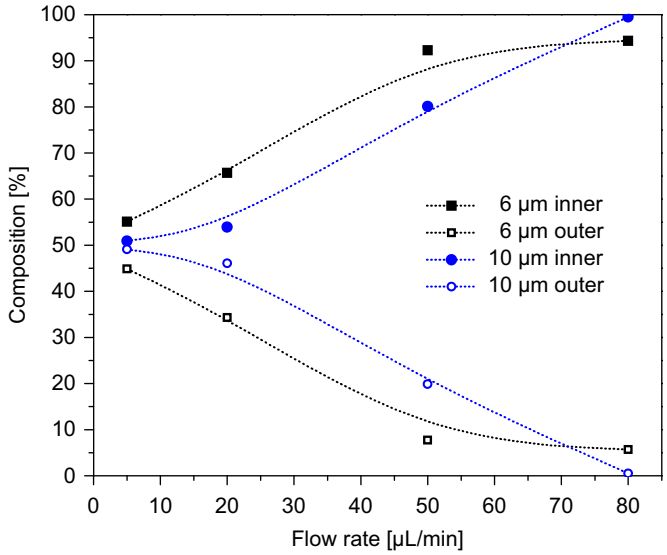

Fig. 5. Relative MMS content in the two separated fluid fractions, collected at different flow rates and with two different particle sizes; note that the curves shown here are merely intended as guides for the eye.

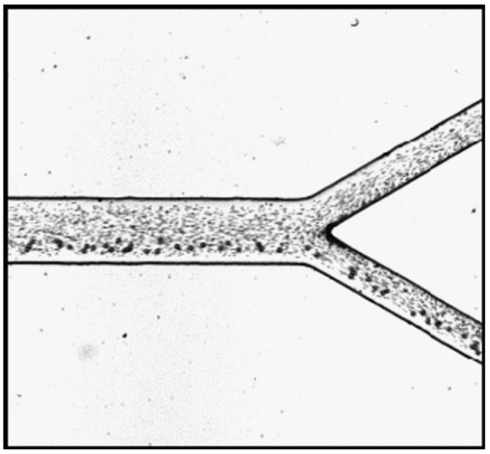

Fig. 6. Distribution of 2 μm and 12 μm particle streams observed at a flow rate of 40 μL/min. All 12 μm particles were found in the inner fraction while more than 50% of the 2 μm particles moved toward the outer outlet.

outlet channel and that the inner channel is wide enough to transport all of the entrained particles.

4.2. Bimodal mixture of monodisperse MMS

As the flow rate through the spiral was increased it was observed that the number of 12 μm MMS found in the sample collected from the inner outlet increased (Fig. 6). Fig. 7a shows the composition of a mixture nominally consisting of 2 μm and 12 μm diameter MMS, as determined by static light scattering. A bimodal distribution is clearly visible, with peaks at 2.05 μm and 12.33 μm. A complete elimination of 12 μm MMS from the outer sample was achieved for flow rates of 50 μL/min (Fig. 7b) or higher, while at the same time only a small amount of the 2 μm MMS was found in the inner sample (Fig. 7c). This experiment demonstrates the concentration of one particle size from a bimodal particle mix.

Looking at this more closely (Fig. 8), the distribution of larger (12 μm) and smaller (2 μm) MMS reveals that the larger particles are equally likely to exit via the two outlets at low flow rates. As the flow rate increases, more and more of the larger diameter MMS move to the inner outlet. At flow rates above 40 μL/min all of the 12 μm MMS appear at the inner outlet (Fig. 8a). The 2 μm diameter particles also start out with equal probabilities for exiting via the two outlets at low flow rates but then increasingly shift toward the outer outlet at higher flow rates. At a flow rate of 60 μL/min about 90% of the smaller MMS are found in the outer sample (Fig. 8b). A further improvement of the separation can be expected for higher flow rates. However, due to technical reasons it is complicated to increase the flow rates above 60 μL/min in the current device. Flow rates higher than 60 μL/min usually led to leakage at the inlet tubing due to the associated high pressure at the chip inlet.

Under the conditions we have examined to date, the complete separation of a bimodal particle mixture into its constituent components has not been possible. We have observed that it is possible to extract samples from the outer outlet that are absolutely free of the larger diameter particles, but samples extracted from the inner outlet always contain some smaller diameter particles (with minimum concentrations of approximately 10%). This incomplete separation might be overcome using an asymmetric splitter. One might also consider running the sample through the fractionation system (or through a chain of fractionation systems) multiple times. After three iterations the proportion of smaller diameter particles collected at the inner outlet should nominally be lower than 0.1% of the total; after five passes this would be reduced to less than 0.001%.

4.3. MMS with a broad size distribution

When a polydisperse suspension of MMS with a broad size distribution is sent through the microfluidic separator, it is expected that larger diameter MMS will move towards the inner fraction. As a consequence the average MMS diameter in the outer fraction will be lower than the mean diameter of particles in the initial sample. This expectation was confirmed through experimentation. The initial sample used for these experiments was analyzed and found to have a mean MMS diameter of 3.56 μm and a standard deviation of ± 2.82 μm.

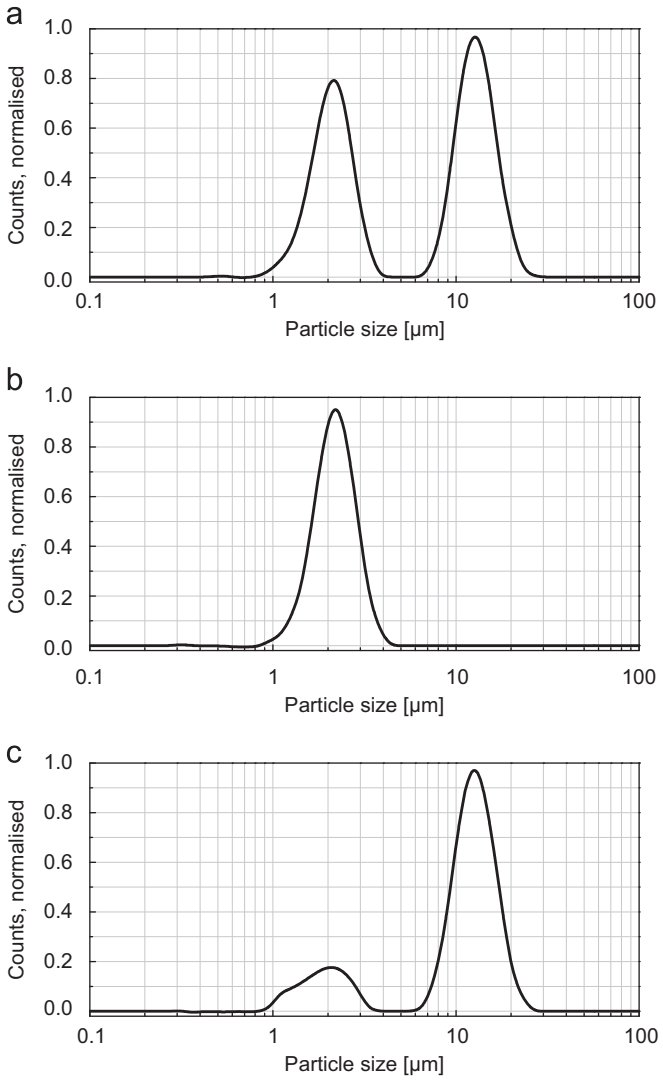

Fig. 7. Particle size distributions determined by static light scattering (a) in the original suspension, (b) in the outer fraction and (c) in the inner fraction collected at a flow rate of 50 μL/min.

Fig. 9 shows that, even at relatively low flow rates, a slight shift of mean particle diameter relative to the initial sample is observed at the two outlets. At a flow rate of 10 μL/min the MMS in the inner fraction exhibit a mean diameter of 3.61 ± 2.53 μm, while those in the outer fraction exhibit a mean diameter of 3.47 ± 2.45 μm. This shift in mean diameter continues to increase with increasing flow rate. At 60 μL/min the mean particle diameters extracted from the inner and outer outlets were 4.21 ± 3.09 μm and 2.74 ± 1.90 μm, respectively.

Usually, a size dependent fractionation is accompanied by a narrowing of the size distribution. However, in our experiments the size distribution during this fractionation changed only slightly. A narrowing of the size distribution can be achieved by consecutive separation runs of the fraction with the desired MMS diameter. This way smaller and larger MMS can be removed from the fraction with the desired mean MMS size which leads to a narrowing of the size distribution.

4.4. Non-magnetic and magnetic microspheres of the same size

In an effort to explore the potential role of density and/or magnetic interactions, we injected a suspension containing equal numbers of non-magnetic (density = 1.10 g/cm^3) and magnetic (density = 1.85 g/cm^3) microspheres with the same characteristic size (5 μm). No discernable (differential) fractionation effect was observed for all investigated flow rates. The obtained fractions from inner and outer outlet show the same solid content and the same magnetization (Table 1). That is, the proportion of magnetic MMS extracted at both outlets was equal to 50% (within the measurement error) for each flow rate at which observations were made. In other words, the samples extracted from both outlets contain the same amount of magnetic and non-magnetic particles; no enrichment of either the magnetic or the non-magnetic component occurred.

These results demonstrate for the first time that the role of density (and magnetic interactions) in determining the equilibrium location of particle streamlines in the fluid are insignificant relative to particle size. The implication is that these fractionation methods ought to be useful for simultaneous separation of neutrally-buoyant and non-neutrally-buoyant particles. Certainly caution is warranted: the range of densities explored in this experiment was relatively small (1.10–2.25 g/cm^3); future investigations probing a broader range of density would be worthwhile.

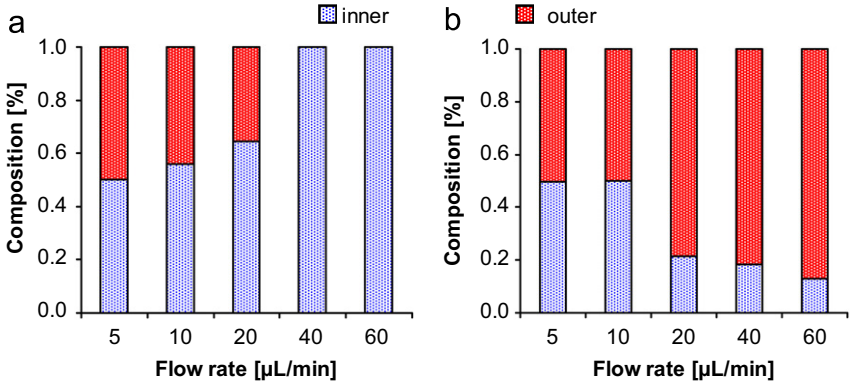

Fig. 8. Experimentally determined probability of finding (a) larger (12 μm) MMS and (b) smaller (2 μm) MMS at the two outlet ports, as a function of flow rate.

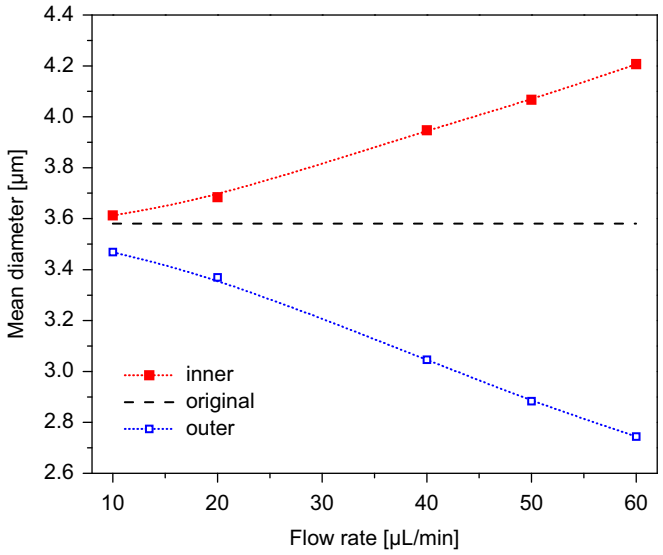

Fig. 9. Mean diameter of particles extracted from the two outlets when a polydisperse suspension is injected into the spiral channel, as a function of flow rate.

Table 1
Distribution of MMS in the samples extracted from the two outlets, as a function of the flow rate. The initial mixture contained equal amounts of magnetic and non-magnetic 5 µm microspheres.

Flow rate [µL/min]	Inner sample [%]	Outer sample [%]
5	49.5	50.5
10	50.6	49.4
20	49.2	50.8
40	51.5	48.5
60	51.8	48.2

Tests were also conducted to investigate the robustness of the Dean-effect fractionation process under influence of a strong uniform magnetic field and a strong magnetic field gradient. As expected, it was observed that proper functioning of the chip was degraded by application of magnetic field gradients. The particle clusters formed in the inlet tubing and at the inlet port are attracted by the magnet toward the channel walls. Due to the large port diameter, the flow in this region is not fast enough for the hydrodynamic forces to overcome the magnetic forces and flush away the agglomerates. As a result, agglomerates grow in size with every new injected particle until the passage is blocked completely. When the magnetic field gradient is removed the clusters break apart and all of the MMS are flushed through the spiral. Even weak magnetic field gradients in the order of 1.5 T/m (at field strengths in the order of 5.5 kA/m) were sufficient to totally block the channel. In contrast to this, when a spatially homogeneous magnetic field of the same strength was applied, no influence on the fractionation process was observed. Even for relatively strong magnetic fields (in the order of 35 kA/m) only a slight tendency of the MMS to form agglomerates (caused by attractive magnetic particle–particle interactions) was observed in the inlet port where the flow velocity is relatively low. These agglomerates (clusters and chains) were broken apart by high Stokes forces once the particles entered the spiral channel, where the velocity of the carrier liquid can be as high as 3 m/s. Note that since the magnetic cores of the MMS used in this study are embedded in a polymer matrix, they do not come into direct contact with each other. The magnetic attraction between the MMS thus tends to be relatively weak. We conclude that this particle separation system can tolerate strong homogeneous magnetic fields, but that the presence of even relatively minor magnetic field gradients at the inlet of the chip must be prevented if they are applied in random directions.

5. Conclusions

We have developed a microfluidic chip that enables the complete recovery of particles from highly diluted particle dispersions. It is able to separate particles showing a bimodal particle size distribution into distinct size fractions based on Dean flow combined with lift forces acting on the particles in a curved microchannel. For a particle suspension with a broad size distribution the chip is able to separate fractions containing particles of different sizes in a continuous process. The size fractions can be chosen simply by adjusting the flow velocity of the carrier fluid.

In the experiments MMS suspension flow rates of 0.3–4.8 mL/h were used for the fractionation, yielding a throughput of 1.5–24 mg MMS per hour for continuous operation. This fractionation method is easily scalable as it is possible to run hundreds of these devices in parallel in order to increase the throughput.

Our experimental investigation proved that the particle density has no influence on the investigated effect and a size dependent fractionation of non-neutrally buoyant particles by means of the presented microfluidic chip is possible.

Furthermore, we showed that this particle separation system can tolerate strong homogeneous magnetic fields. Clusters and chains formed in the inlet are eliminated in the channel due to the high flow velocity of the sample. In contrast, the chip is very sensitive to magnetic gradients because the attracting force acting on the particles led to the formation of clusters which are restrained in the inlet and this can cause an occlusion of the chip; this occurred already at very low magnetic gradients.

This separation method can be used to extract particles above a particular size (collected in the inner phase) or to remove particles above a particular size (sample collected in the outer phase). A suspension of particles with a narrow size distribution can be achieved through a sequence of separation steps. This method is therefore adequate for the high-throughput fractionation of a sample of polydisperse MMS to achieve MMS with a narrow size distribution, as required for magnetic drug targeting. Theoretically, the Dean effect is also suitable for the fractionation of objects much smaller than 1 µm (e.g., nanoparticles) but the realization of the necessary flow rate in the downscaled channels would be very challenging due to the associated high flow resistance that would require very high pressures.

Acknowledgments

The authors thank Dr. Thomas Henkel (IPHT) for fruitful discussions and critical reading of the manuscript. We thank chemicell GmbH, Berlin, Germany, and micromod Partikeltechnologie GmbH, Rostock, Germany, for MMS samples. The work was funded by the International Bureau of the Federal Ministry of Education and Research of Germany and by a fellowship within the Postdoc-Program of the German Academic Exchange Service (DAAD). The authors also acknowledge equipment funding from the Canadian Foundation for Innovation (CFI) and funding from the British Columbia Innovation Council (BCIC) through a scholarship. Furthermore, we acknowledge support from NSERC's Discovery Grant program.

References

[1] W. Andrä, U.O. Häfeli, R. Hergt, R. Misri, Application of magnetic particles in medicine and biology, in: H. Kronmüller, S. Parkin (Eds.), The Handbook of Magnetism and Advanced Magnetic Materials, vol. 4—Novel Materials, John Wiley & Sons Ltd., Chichester, 2007, pp. 2536–2568.

[2] V.P. Torchilin, M.I. Papisov, N.M. Orekhova, A.A. Belyaev, A.D. Petrov, S.E. Ragimov, Magnetically driven thrombolytic preparation containing immobilized streptokinase-targeted transport and action, Haemostasis 18 (1988) 113–116.

[3] M.D. Torno, M.D. Kaminski, Y. Xie, R.E. Meyers, C.J. Mertz, X. Liu, W.D. O'Brien Jr., A.J. Rosengart, Improvement of in vitro thrombolysis employing magnetically-guided microspheres, Thrombosis Research 121 (2008) 799–811.

[4] U.O. Häfeli, Magnetic nano- and microparticles for targeted drug delivery, in: R. Arshady, K. Kono (Eds.), Smart Nanoparticles in Nanomedicine—the MML Series, Kentus Books, London, 2006, pp. 77–126.

[5] H. Zhao, J. Gagnon, U.O. Häfeli, Process and formulation variables in the preparation of injectable and biodegradable magnetic microspheres, Biomagnetic Research and Technology 5 (2007) 2.

[6] R. Rosensweig, Ferrohydrodynamics, Cambridge University Press, Cambridge, 1985.

[7] N. Willmott, J. Daly, Microspheres and Regional Cancer Therapy, CRC Press, Boca Raton, 1994.

[8] L. Zeng, L. An, X. Wu, Modeling drug–carrier interaction in the drug release from nanocarriers, Journal of Drug Delivery (2011)http://dx.doi.org/10.1155/2011/370308.

[9] J.F. Berret, O. Sandre, A. Mauger, Size distribution of superparamagnetic particles determined by magnetic sedimentation, Langmuir 23 (2007) 2993–2999.

[10] S. Dutz, J.H. Clement, D. Eberbeck, T. Gelbrich, R. Hergt, R. Muller, J. Wotschadlo, M. Zeisberger, Ferrofluids of magnetic multicore nanoparticles for biomedical applications, Journal of Magnetism and Magnetic Materials 321 (2009) 1501–1504.

[11] R. Gerber, Magnetic filtration of ultra-fine particles, IEEE Transactions on Magnetics 20 (1984) 1159–1164.

[12] G. Glöckl, R. Hergt, M. Zeisberger, S. Dutz, S. Nagel, W. Weitschies, The effect of field parameters, nanoparticle properties and immobilization on the specific heating power in magnetic particle hyperthermia, Journal of Physics—Condensed Matter 18 (2006) 2935–2949.

[13] J. Chatterjee, Y. Haik, C.J. Chen, Size dependent magnetic properties of iron oxide nanoparticles, Journal of Magnetism and Magnetic Materials 257 (2003) 113–118.

[14] S. Thurm, S. Odenbach, Magnetic separation of ferrofluids, Journal of Magnetism and Magnetic Materials 252 (2002) 247–249.

[15] B. Chanteau, J. Fresnais, J.F. Berret, Electrosteric enhanced stability of functional sub-10 nm cerium and iron oxide particles in cell culture medium, Langmuir 25 (2009) 9064–9070.

[16] M. Yamada, M. Seki, Hydrodynamic filtration for on-chip particle concentration and classification utilizing microfluidics, Lab on a Chip 5 (2005) 1233–1239.

[17] B. Mustin, B. Stoeber, Deposition of particles from polydisperse suspensions in microfluidic systems, Microfluidics and Nanofluidics (2010)http://dx.doi.org/10.1007/s10404.

[18] D. Huh, J.H. Bahng, Y.B. Ling, H.H. Wei, O.D. Kripfgans, J.B. Fowlkes, J.B. Grotberg, S. Takayama, Gravity-driven microfluidic particle sorting device with hydrodynamic separation amplification, Analytical Chemistry 79 (2007) 1369–1376.

[19] T. Laurell, F. Petersson, A. Nilsson, Chip integrated strategies for acoustic separation and manipulation of cells and particles, Chemical Society Reviews 36 (2007) 492–506.

[20] G. Milne, D. Rhodes, M. MacDonald, K. Dholakia, Fractionation of polydisperse colloid with acousto-optically generated potential energy landscapes, Optics Letters 32 (2007) 1144–1146.

[21] M. Zborowski, L.P. Sun, L.R. Moore, P.S. Williams, J.J. Chalmers, Continuous cell separation using novel magnetic quadrupole flow sorter, Journal of Magnetism and Magnetic Materials 194 (1999) 224–230.

[22] F. Carpino, M. Zborowski, P.S. Williams, Quadrupole magnetic field-flow fractionation: a novel technique for the characterization of magnetic nanoparticles, Journal of Magnetism and Magnetic Materials 311 (2007) 383–387.

[23] N. Pamme, J.C.T. Eijkel, A. Manz, On-chip free-flow magnetophoresis: separation and detection of mixtures of magnetic particles in continuous flow, Journal of Magnetism and Magnetic Materials 307 (2006) 237–244.

[24] K. Smistrup, O. Hansen, H. Bruus, M.F. Hansen, Magnetic separation in microfluidic systems using microfabricated electromagnets—experiments and simulations, Journal of Magnetism and Magnetic Materials 293 (2005) 597–604.

[25] N. Pamme, Continuous flow separations in microfluidic devices, Lab on a Chip 7 (2007) 1644–1659.

[26] J.D. Adams, H.T. Soh, Perspectives on utilizing unique features of microfluidics technology for particle and cell sorting, Journal of the Association for Laboratory Automation 14 (2009) 331–340.

[27] W.R. Dean, Note on the motion of fluid in a curved pipe, Philosophical Magazine (Ser. 7) 4 (1927) 208–223.

[28] W.R. Dean, The stream-line motion of fluid in a curved pipe, Philosophical Magazine (Ser. 7) 5 (1928) 673–695.

[29] D.R. Gossett, D. Di Carlo, Particle focusing mechanisms in curving confined flows, Analytical Chemistry 81 (2009) 8459–8465.

[30] E. Sollier, H. Rostaing, P. Pouteau, Y. Fouillet, J.L. Achard, Passive microfluidic devices for plasma extraction from whole human blood, Sensors and Actuators B—Chemical 141 (2009) 617–624.

[31] J. Seo, M.H. Lean, A. Kole, Membraneless microseparation by asymmetry in curvilinear laminar flows, Journal of Chromatography A 1162 (2007) 126–131.

[32] A.A.S. Bhagat, S.S. Kuntaegowdanahalli, I. Papautsky, Continuous particle separation in spiral microchannels using Dean flows and differential migration, Lab on a Chip 8 (2008) 1906–1914.

[33] S.S. Kuntaegowdanahalli, A.A.S. Bhagat, G. Kumar, I. Papautsky, Inertial microfluidics for continuous particle separation in spiral microchannels, Lab on a Chip 9 (2009) 2973–2980.

[34] R. Eichhorn, S. Small, Experiments on the lift and drag of spheres suspended in a Poiseuille flow, Journal of Fluid Mechanics 20 (1964) 513–527.

[35] D. Di Carlo, D. Irimia, R.G. Tompkins, M. Toner, Continuous inertial focusing, ordering, and separation of particles in microchannels, Proceedings of the National Academy of Sciences of the United States of America 104 (2007) 18892–18897.

[36] G. Segre, A. Silberberg, Radial particle displacements in Poiseuille flow of suspensions, Nature 189 (1961) 209–210.